AN ITERATIVE SUBPROBLEM METHOD FOR THIN SHELL FINITE ELEMENT MAGNETIC MODELS

Dang Quoc Vuong

Hanoi University of Science and Technology; vuong.dangquoc@hust.edu.vn

Abstract - An iterative sub-problem method for thin shell finite element magnetic models is herein performed to correct the inaccuracies near edges and corners arising from thin shell models (e.g., cover of transformers, thin shells, steel laminations). Volume thin regions are replaced by surfaces but neglect border effects in the vicinity of their edges and corners. This leads to errors for solving the thin shell finite element magnetic models. A sub-problem method allows users to split a complete problem (e.g., a system composed of stranded inductors and conducting and magnetic possibly thin regions) into a series of sub-problems that define a sequence of changes, with the complete solution expressed as the sum of the sub-problem solutions. Each sub-problem is solved on its own domain and mesh, which facilitates meshing and may increase computational efficiency.

Key words - Eddy current; finite element method (FEM); sub-problem; sub-problem method (SPM); thin shell (TS)

1. Introduction

Thin shell (TS) finite element (FE) models [1-2] are commonly used to avoid volumetrically meshing thin regions (Figure 1, *left*). Indeed, the fields in the thin regions are approximated by *priori* known 1-D analytical distributions, that generally neglect end and curvature effects (Figure 1, *right*). Their interior is thus not meshed and is rather extracted from the studied domain, being reduced to a zero-thickness double layer with interface conditions (IC) linked to the inner analytical distributions [1-2]. These ICs lead to inaccuracies on the computation of local electromagnetic quantities in the vicinity of geometrical discontinuities. Such inaccuracies increase with the thickness, and is exacerbated for quadratic quantities like force and Joule losses, which are often the primary quantities of interest.

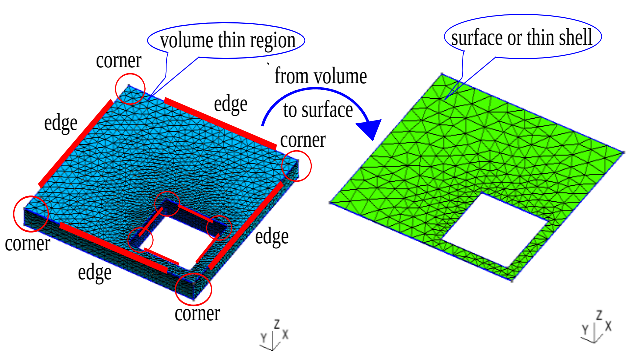

Figure 1. *From volume thin region to thin shell model*

In order to cope with this problem, the authors have recently proposed a sub-problem method (SPM) for correcting edge and corner errors and to simplify meshing in **one-way coupling** sub-problems (SPs), where no iteration between the SPs is necessary [3-6].

In this paper, the SPM is extended to correct the inherent inaccuracies of the field distributions and Joules edge and corner errors in **two-coupling** SPs, where each solution is influenced by all the others, which thus must be included in an iterative process. The method allows users to correct the inherent inaccuracies of the filed distributions and Joule losses near edges and corners appearing from the TS models.

In the proposed SP strategy [3-5], a reduced problem with only inductors is first solved on a simplified mesh without thin and volume regions. Its solution gives surface sources (SSs) as ICs for added TS regions, and volume sources (VSs) for possible added volume regions. The TS solution is further improved by a volume correction via SSs and VSs that overcome at the TS assumptions, respectively suppressing the TS model and adding the volume model.

2. Iterative sequence of sub-problems

2.1. Canonical magneto-dynamic or static problem

A canonical magneto-dynamic problem i, to be solved at step i of the SPM, is defined in a domain Ω_i, with boundary $\partial\Omega_i = \Gamma_i = \Gamma_{h,i} \cup \Gamma_{b,i}$. The eddy current conducting part of Ω_i is denoted $\Omega_{c,i}$ and the non-conducting one $\Omega_{c,i}{}^C$, with $\Omega_i = \Omega_{c,i} \cup \Omega_{c,i}{}^C$. Stranded inductors belong to $\Omega_{c,i}{}^C$, whereas massive inductors belong to $\Omega_{c,i}$. The equations, material relations and boundary conditions (BCs) of SP i are

$$\text{curl}\, \boldsymbol{h}_i = \boldsymbol{j}_i,\ \text{div}\, \boldsymbol{b}_i = 0,\ \text{curl}\, \boldsymbol{e}_i = -\, \partial_t\, \boldsymbol{b}_i \qquad \text{(1a-b-c)}$$

$$\boldsymbol{h}_i = \mu_i{}^{-1}\, \boldsymbol{b}_i + \boldsymbol{h}_{s,i},\ \boldsymbol{j}_i = \sigma_i\, \boldsymbol{e}_i + \boldsymbol{j}_{s,I} \qquad \text{(2a-b)}$$

$$\boldsymbol{n} \times \boldsymbol{h} = \boldsymbol{j}_{f,i},\ \boldsymbol{n} \times \boldsymbol{b}_i|_{\Gamma b,i} = \boldsymbol{f}_{f,i}, \qquad \text{(3a-b)}$$

$$\boldsymbol{n} \times \boldsymbol{e}_i|_{\Gamma e,i \cup \Gamma b,i} = \boldsymbol{k}_{f,i} \qquad (4)$$

where $\boldsymbol{h}_i$ is the magnetic field, $\boldsymbol{b}_i$ is the magnetic flux density, $\boldsymbol{e}_i$ is the electric field, $\boldsymbol{j}_i$ is the electric current density, μ_i is the magnetic permeability, σ_i is the electric conductivity and $\boldsymbol{n}$ is the unit normal exterior to Ω_i. The fields $\boldsymbol{j}_{f,i}$ and $\boldsymbol{k}_{f,i}$ in (3a) and (3b) are surface sources (SSs) and generally equal zero for classical homogeneous BCs. Equations (1b-c) are fulfilled via the definition of a magnetic vector potential $\boldsymbol{a}_i$ and an electric scalar potential v_i, leading to the $\boldsymbol{a}_i$-formulation, with

$$\text{curl}\, \boldsymbol{a}_i = \boldsymbol{b}_i,\ \boldsymbol{e}_i = -\partial_t\, \boldsymbol{a}_i - \text{grad}\, v_i,\ \boldsymbol{n} \times \boldsymbol{a}_i|_{\Gamma_{i,b}} = \boldsymbol{a}_{f,i}. \qquad \text{(5a-b-c)}$$

For various purposes, also for a TS representation, some paired portions of Γ_i can define double layers, with the thin region in between exterior to Ω_i [1]-[3]. They are denoted $\gamma_i{}^+$ and $\gamma_i{}^-$ and are geometrically defined as a single surface γ_i with ICs, fixing the discontinuities $[\cdot]_{\gamma_i} = \cdot|_{\gamma^+} - \cdot\,|_{\gamma_i^-}$).

$$[\boldsymbol{n}\times\boldsymbol{h}_i]_{\gamma_i},\ [\boldsymbol{n}\times\boldsymbol{b}_i]_{\gamma_i},\ [\boldsymbol{n}\times\boldsymbol{e}_i]_{\gamma_i} \text{and } [\boldsymbol{n}\times\boldsymbol{a}_i]_{\gamma_{ip}}. \quad (6a\text{-}b\text{-}c\text{-}d)$$

With the definitions $(\boldsymbol{n}_{\gamma_i}\equiv\boldsymbol{n}|_{\gamma_i}) = -(\boldsymbol{n}^+ \equiv \boldsymbol{n}|_{\gamma_i^+}) = (\boldsymbol{n}^- \equiv \boldsymbol{n}|_{\gamma_i^-})$ for the normal $\boldsymbol{n}$ in different contexts, one has, e.g. for (6a),

$$[\boldsymbol{n}\times\boldsymbol{h}_i]_{\gamma_i} = \boldsymbol{n}_{\gamma_i}\times\boldsymbol{h}_i|_{\gamma_i^+} - \boldsymbol{n}_{\gamma_i}\times\boldsymbol{h}_p|_{\gamma_i^-}$$

$$= -(\boldsymbol{n}^+\times\boldsymbol{h}_i|_{\gamma_i^+} - \boldsymbol{n}^-\times\boldsymbol{h}_i|_{\gamma_i^-}). \quad (7)$$

The field $\boldsymbol{h}_{s,i}$ and $\boldsymbol{j}_{s,i}$ and in (2a) and (2b) are volume sources (VSs) that can be used for expressing changes of a material property in a volume region [3]. The changes of materials in a region, from SPu($i = u$) to SPp($i = p$) are defined via VSs $\boldsymbol{h}_{s,p}$ and $\boldsymbol{j}_{s,p}$, i.e.

$$\boldsymbol{h}_{s,p} = (\mu_p^{-1} - \mu_u^{-1})\, \boldsymbol{b}_u,\ \boldsymbol{j}_{s,p} = (\sigma_p - \sigma_u)\, \boldsymbol{e}_u, \quad (8a\text{-}b)$$

for the total fields to be related by the updated relations $\boldsymbol{h}_u + \boldsymbol{h}_p = \mu_p^{-1}(\boldsymbol{b}_u + \boldsymbol{b}_p)$ and $\boldsymbol{j}_u + \boldsymbol{j}_p = \sigma_p(\boldsymbol{e}_u + \boldsymbol{e}_p)$.

The surface fields $\boldsymbol{j}_{f,i}$, $\boldsymbol{f}_{f,i}$ and $\boldsymbol{k}_{f,i}$ in (3a-b) and (4), and $\boldsymbol{a}_{f,i}$ in (5c), are generally zero for classical homogeneous BCs. The discontinuities (6a-d) are also generally zero for common continuous field traces. If nonzero, they define possible SSs that account for particular phenomena occurring in the thin region between γ_i^+ and γ_i^- [5]-[9]. This is the case when some field traces in a SPu are forced to be discontinuous. The continuity has to be recovered after a correction via a SPp. The SSs in SPp are thus to be fixed as the opposite of the trace solution of SPu.

2.2. Series of coupled sub-problems

The solution $\boldsymbol{x}(\boldsymbol{x}\equiv \boldsymbol{h}, \boldsymbol{b}, \boldsymbol{e}, \boldsymbol{j}\ldots)$ of a complete problem is to be expressed as the sum of SP solutions $\boldsymbol{x}_i$ supported by different meshes [4]. An appropriate series of SPs is worth being defined via successive model refinements of an initially simplified model. Physical considerations usually help to construct a series. For an ordered set $P$of SPs, the summation of their solutions gives the total solution, i.e.

$$\mathbf{x} = \textstyle\sum_{i\in P} \boldsymbol{x}_i \text{ with } \mathbf{x}\equiv \mathbf{h}, \mathbf{b}, \mathbf{e}, \mathbf{j}\ldots$$

Each SP is governed by static or dynamic equations and constrained with SSs (3a-b) and (4c), and VSs (2a-b). As a consequence, each SP i is influenced by all the other SPs q in P to calculate each solution $\boldsymbol{x}_i$ as a series of corrections $\boldsymbol{x}_{i,j}$, i.e.

$$\lim_{n\to\infty} \boldsymbol{x}_i^{\,n} = \boldsymbol{x} = \textstyle\sum_{i\in P} \boldsymbol{x}_{i,j}.$$

The total solution at iteration n is thus

$$\boldsymbol{x}^n = \textstyle\sum_{i\in P} \boldsymbol{x}_i^{\,n} = \sum_{i\in P}\sum_{j=1}^{n} \boldsymbol{x}_{i,j}.$$

The error ϵ^n of a solution $\boldsymbol{x}^n$ is defined by

$$\epsilon^n = \frac{\|\boldsymbol{x}^n - \boldsymbol{x}_{\text{reference}}\|}{\|\boldsymbol{x}_{\text{reference}}\|}$$

where $\boldsymbol{x}_{\text{reference}}$ is a reference solution (calultated for a classical numerical method). However, the reference solution is usually not known. Thus, an estimated error $\epsilon^n_{\text{estimated}}$ of a solution $\boldsymbol{x}^n$ at iteration n has to be defined, e.g. as

$$\epsilon^n_{\text{estimated}} = \frac{\|\boldsymbol{x}^n - \boldsymbol{x}^{n-1}\|}{\|\boldsymbol{x}^n\|}$$

The computation of the conversions $\boldsymbol{x}_{i,j}$ in a SP $_{i,j}$ (SP$_i$ with particular constraints at iteration n) is kept on till convergence up to a desired accuracy. Each correction must account for the influence of all the previous corrections $\boldsymbol{x}_{i,j}$ of other SPs, with j the last iteration index for which a correction is known, i.e. $j = n$ or $n - 1$. Initial solutions $\boldsymbol{x}_i^0$ are set to zero.

2.3. Sub-problems: Two-way coupling

The coupled SP sequences are considered in several SPs:

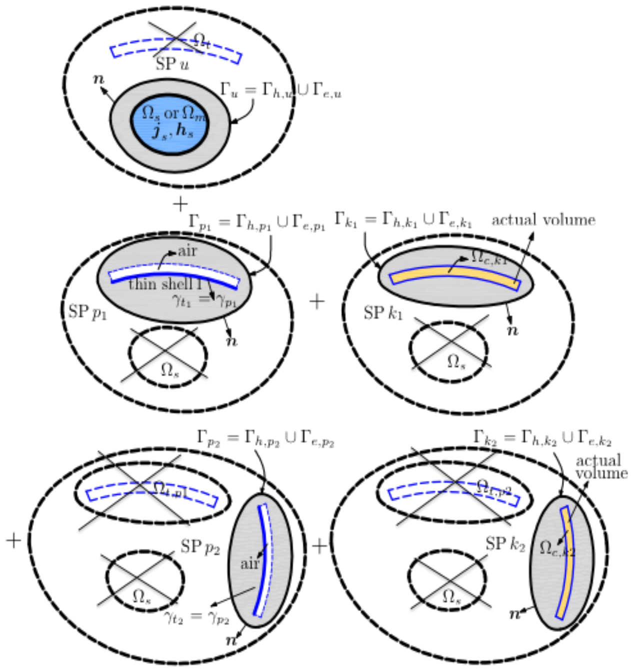

Figure 2. *Decomposition of a complete problem into five SPs:SP u +SPp_1 +SPk_1 + SP p_2 + SPk_2*

A problem (SP u) involving current driven stranded inductors is first solved on a simplified mesh without any thin regions in Figure 2. Its solution gives surface sources (SSs) for the added TS 1 (SP p_1) (Figure 2, *middle left*) through TS ICs based on 1-D approximations. The solution of SP p_1 is then corrected by a correction problem (SP k_1) (Figure 2, *middle right*) via SSs and volume sources (VSs), that suppress the TS representation and simultaneously add the actual volume of the thin region. Two new added SPs are respectively called TS 2 (SPp_2) (Figure 2, *bottom left*) and volume correction 2 (SPk_2) (Figure 2, *bottom right*). Here, SPp_2 and SPk_2 are independently solved in their own domain that do not include all previous SP regions anymore. Once obtained, the solutions of all the previous SPs then give SSs for the new added TS SPp_2 through ICS [1-2]. The TS solution of SPp_2 is then corrected by an SPk_2, that also suppresses the TS representation and simultaneously add the sources of SPp_1 and SPk_1. SP u need no artificial sources and is therefore not influenced. This leads to changes of all the previous corrections [3-6]. Therefore, each solution has to be calculated as a series of corrections by iterating between SPs.

3. Finite Element Weak Formulation

3.1. Magnetic Vector Potential Formulation

The weak $\boldsymbol{b}_i$ -formulation (in terms of $\boldsymbol{a}_i$) of SP i ($i \equiv u$, p or k) is obtained from the weak form of the Ampère equation (1a), i.e. [3], [4]

$$(\mu_i^{-1}\operatorname{curl}\boldsymbol{a}_i, \operatorname{curl}\boldsymbol{a}_i')_{\Omega_i} + (\boldsymbol{h}_{s,i}, \operatorname{curl}\boldsymbol{a}_i')_{\Omega_i} + (\boldsymbol{j}_{s,i}, \boldsymbol{a}_i')_{\Omega_i}$$
$$+ (\sigma_i \partial_t \boldsymbol{a}_i, \boldsymbol{a}_i')_{\Omega_i} + < \boldsymbol{n} \times \boldsymbol{h}_i, \boldsymbol{a}_i' >_{\Gamma_{h,i} - \Gamma_{t,i}} + < [\boldsymbol{n} \times \boldsymbol{h}_i]_{\Gamma_{t,i}}, \boldsymbol{a}_i' >_{\Gamma_{t,i}}$$
$$= (\boldsymbol{j}_{s,i}, \boldsymbol{a}_i')_{\Omega_i}, \forall \boldsymbol{a}_i' \in F_i^1(\Omega_i) \tag{9}$$

where $F_i^1(\Omega_i)$ is a curl-conform function space defined in Ω_i, gauged in $\Omega_{c,i}^C$, and containing the basis functions for $\boldsymbol{a}$ as well as for the test function $\boldsymbol{a}_i'$ (at the discrete level, this space is defined by edge FEs; the gauge is based on the tree-co-tree technique); $(\cdot,\cdot)_\Omega$ and $<\cdot,\cdot>_\Gamma$ respectively denote a volume integral in Ω and a surface integral on Γ of the product of their vector field arguments. The surface integral term on $\Gamma_{h,i}$ accounts for natural BCs of type (3a), usually zero. At the discrete level, the required meshes for each SP i in the SPM totally differ.

3.2. Inductor alone – SP u

The weak form of an SP u with the inductor alone is first solved via the first and last volume integrals in (9) ($i \equiv u$) where $\boldsymbol{j}_{s,u}$ is the fixed current density in on Ω_S.

3.3. Thin shell FE model- SP$_p$

The TS model is defined via the term $< [\boldsymbol{n} \times \boldsymbol{h}_p]_{\gamma_p}, \boldsymbol{a}_{d,p}' >_{\gamma_p}$ in (9)($i \equiv p$). The test function $\boldsymbol{a}_p'$ is split into continuous and discontinuous parts $\boldsymbol{a}'_{c,p}$ and $\boldsymbol{a}'_{d,p}$ (with $\boldsymbol{a}'_{d,p}$ zero on γ^-_p) [2]. One thus has

$$< [\boldsymbol{n} \times \boldsymbol{h}_p]_{\gamma_p}, \boldsymbol{a}_p' >_{\gamma_p} = < [\boldsymbol{n} \times \boldsymbol{h}_p]_{\gamma_p}, \boldsymbol{a}_{c,p}' >_{\gamma_p} +$$
$$< \boldsymbol{n} \times \boldsymbol{h}_p |_{\gamma^+_p}, \boldsymbol{a}_{d,p}' >_{\gamma^+_p} \tag{10}$$

The terms of the right hand side of (10) are developed using (4) and (7) respectively, i.e.

$$< [\boldsymbol{n} \times \boldsymbol{h}_p]_{\gamma_p}, \boldsymbol{a}_{c,p}' >_{\gamma_p} = < [\boldsymbol{n} \times \boldsymbol{h}]_{\gamma_p}, \boldsymbol{a}_{c,p}' >_{\gamma_p}$$
$$= < \sigma_p \beta_p \partial_t (2\boldsymbol{a}_{c,p} + \boldsymbol{a}_{d,p}), \boldsymbol{a}_{c,p}' >_{\gamma_p} \tag{11}$$

$$< [\boldsymbol{n} \times \boldsymbol{h}_p]_{\gamma^+_p}, \boldsymbol{a}_{d,p}' >_{\gamma_p} = - < \boldsymbol{n} \times \boldsymbol{h}_u |_{\gamma^+_p}, \boldsymbol{a}_{d,p}' >_{\gamma^+_p} +$$
$$\frac{1}{2} < \sigma_p \beta_p \partial_t (2\boldsymbol{a}_{c,p} + \boldsymbol{a}_{d,p}) + \frac{1}{\sigma_p \beta_p}, \boldsymbol{a}_{d,p}' >_{\gamma_p} \tag{12}$$

The last surface integral term in (12) is related to a SS that can be naturally expressed via the weak formulation of SP u (9), i.e.

$$- < \boldsymbol{n} \times \boldsymbol{h}_u |_{\gamma^+_p}, \boldsymbol{a}_{d,p}' >_{\gamma^+_p} = (\mu_u^{-1} \operatorname{curl}\boldsymbol{a}_u, \operatorname{curl}\boldsymbol{a}_{d,p}')_{\Omega^+_p} \tag{13}$$

At the discrete level, the volume integral in (13) is thus limited to a single layer of FEs on the side Ω^+_p touching $\gamma_p{}^+$, because it involves only the associated trace $\boldsymbol{n} \times \boldsymbol{a}_{d,p}'|_{\gamma^+_p}$. Also, the source $\boldsymbol{a}_u$, initially in the mesh of SP u, has to be projected on the mesh of SP p, using a projection method [5], [6].

3.4. TS Correction- VSs in the Actual Volume Shell and SSs for Suppressing the TS representation - SP k

The TS SP p solution is then corrected by SP k via the volume integrals $(\boldsymbol{h}_{s,p}, \operatorname{curl}\boldsymbol{a}')_{\Omega_p}$ and $(\boldsymbol{j}_{s,p}, \boldsymbol{a}')_{\Omega_p}$ in (11). The VSs $\boldsymbol{j}_{s,k}$ and $\boldsymbol{h}_{s,k}$ are given in (9).

Simultaneously to the VSs in (9), SSs have to suppress the TS discontinuities, with ICs to be defined as

$$[\boldsymbol{n} \times \boldsymbol{h}_k]_{\gamma_k} = -[\boldsymbol{n} \times \boldsymbol{h}_p]_{\gamma_k} \text{ and } [\boldsymbol{n} \times a]_{\gamma_k} = -[\boldsymbol{n} \times a_p]_{\gamma_k}.$$

The trace discontinuity $[\boldsymbol{n} \times \boldsymbol{h}_k]_{\gamma_k}$ occurs in (9) via

$$< [\boldsymbol{n} \times \boldsymbol{h}_k]_{\gamma_k}, \boldsymbol{a}_k' >_{\gamma_p} = - < [\boldsymbol{n} \times \boldsymbol{h}_p]_{\gamma_k}, \boldsymbol{a}_k' >_{\gamma_k} \tag{14}$$

and can be weakly evaluated from a volume integral from SP p similar to (13). However, directly using the explicit form (4) for $[\boldsymbol{n} \times \boldsymbol{h}_p]_{\gamma_k}$ gives the same contribution, which is thus preferred.

4. Applications

Let us consider a convergence test of the **two-way** coupling with a simple didactic example (f = 50Hz, $\mu_r = 1, \sigma = 59$ MS/m) (Figure 3).

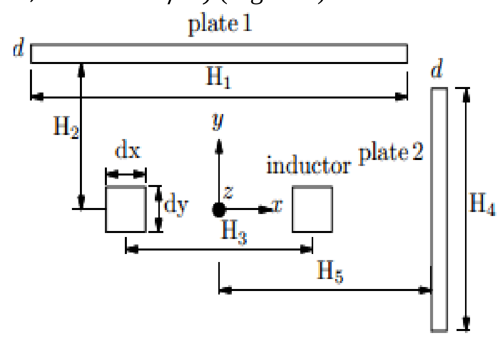

Figure 3. *2-D geometry of an inductor and two plates (d = 5mm, H1 = 120mm, H2 = H3 = 45mm, H4 = 80mm, H5 = 67.5mm, dx = dy = 12mm)*

$$\xrightarrow{\textbf{Convergence}} \boldsymbol{a} = \sum_{i \in P} \boldsymbol{a_i} = \boldsymbol{a_{u,0}} + \sum_{j=1}^{n} \boldsymbol{a_{p1,j}} + \sum_{j=1}^{n} \boldsymbol{a_{k1,j}}$$
$$+ \sum_{j=1}^{n} a_{p2,j} + \sum_{j=1}^{n} a_{k2,j}$$

The test at hand is considered in five SPs. It is first solved via an SP u with the stranded inductor alone, then adding a TS FE SP p_1 that does not include the stranded inductor anymore. An SP k_1 then replaces the TS SPp_1 with an actual volume covering the plate 1. Next, another TS SP p_2 is added. An SP k_2 eventually replaces the TS SP p_2 with another actual volume covering the plate 2. In the correction process of SP p_1, the fields generated by SP p_2 and SP k_2 are reaction fields that influence the source solutions calculated from previous SPp_1. This means that some iterations between the SPs are required to determine an accurate solution considered as a series of corrections.

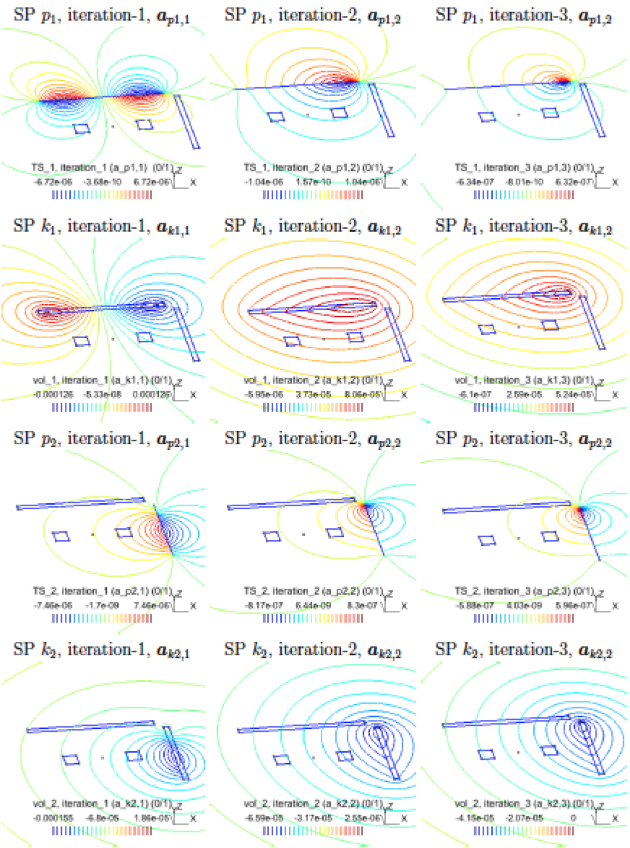

Figure 4. *Flux lines of the z-component of the magnetic vector potential corrections (real part) calculated in each SP, i.e. SPp_1, SPk_1, SPp_2 and SPk_2, with three interations. SPp_1 is chosen as the reference of source SP. The imaginary part presents an analogous behavior*

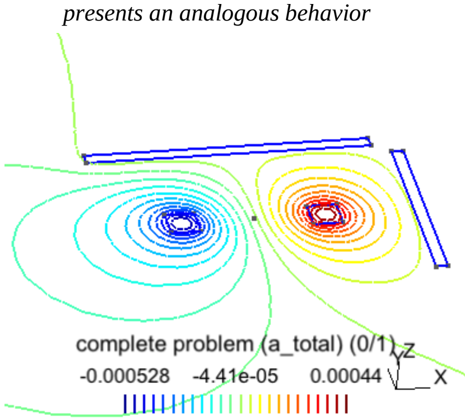

Figure 5. *The total solutionsaof SPs after convergence*

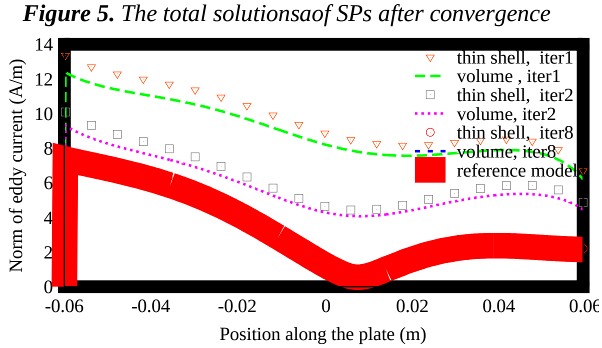

Figure 6. *The norm of eddy current density ||j|| (A/m) along the plate 1 at the different iterations*

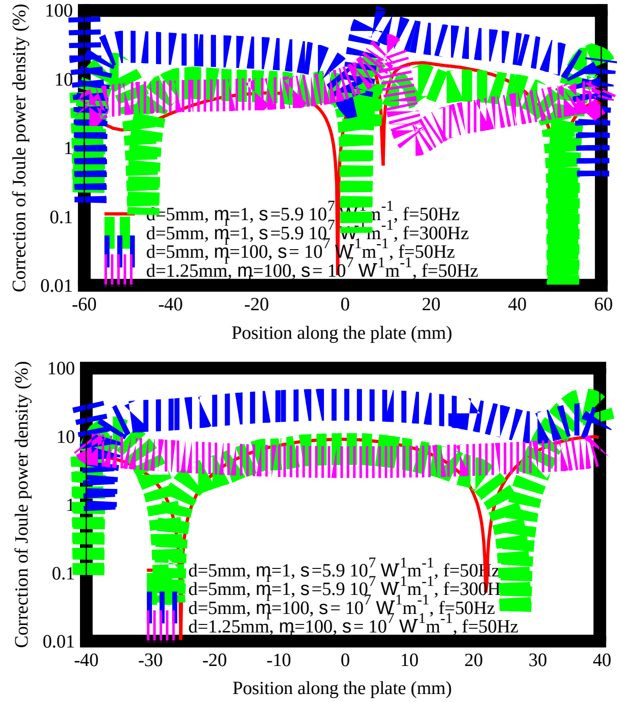

Figure 7. *Relative correction of the Joule power density along the plate 1 (top) and the plate 2 (bottom) for the two-way coupling, with effects of d, μ_r, σ and f*

Table 1. *Comparation of direct FEM and one-way/two-way SPM. The solutions of each SP of each mesh ($\mathcal{M}_u, \mathcal{M}_{p_1}, \mathcal{M}_{p_2}, \mathcal{M}_{k_1}$ and $\mathcal{M}_{k_2}$) are shown in Figure 5 leading to the solution of linear system of n_u, n_p and n_k equations, respectively. The number of iterations of two-way n. coupling is n*

Variation of position of the plate	Classical method	Subproblem method	
	Full problem	One-way coupling	One-way coupling
N times	- *N* times full mesh $\mathcal{M}$ - *N* solutions of $n_f \times n_f$ LS	SP *u*: - 1 times full mesh $\mathcal{M}$ - 1 solution of $n_u \times n_u$ LS SP *p*: - 1 times full mesh $\mathcal{M}$ - 2 solution of $n_p \times n_p$ LS SP *k*: - 1 times full mesh $\mathcal{M}$ - 2 solution of $n_k \times n_k$ LS	SP *u*: - 1 times full mesh $\mathcal{M}$ - 1 solution of $n_u \times n_u$ LS SP p_1: - 1 times full mesh $\mathcal{M}_{p1}$ - $2 \times n$ solution of $n_{p1} \times n_{p1}$ LS SP k_1: - 1 times full mesh $\mathcal{M}_{k1}$ - $2 \times n$ solution of $n_{k1} \times n_{k1}$ LS SP p_2: - 1 times full mesh $\mathcal{M}_{p2}$ - $2 \times n$ solution of $n_{p2} \times n_{p2}$ LS SP k_2: - 1 times full mesh $\mathcal{M}_{k2}$ - $2 \times n$ solution of $n_{k2} \times n_{k2}$ LS

Figure 4 illustrates an iterative process (with three iterations) of four SPs (i.e. SPp_1, SPk_1, SPp_2 and SPk_2) for the magnetic vector potential $\boldsymbol{a}$, where SPp_1 is chosen as a source SP. Note that the source problem SP *u* does not need to be corrected, because it only contains the current driven inductor and needs no SS or VS. Figure 5 gives the tolerance of the total solution $\boldsymbol{a}$ of the convergence (8 iterations). Figure 6 represents the convergence of the volume correction SPk_1 along the plate 1, for different iterations. The TS solution is also pointed out as a function of the number of iterations. The error on the Joule power density in the plate 1 and plate 2 depends on several parameters, as depicted in Figure 7. It can reach 60% in the end region of plate 1 (Figure 7, *top*) and 40% in the end region of plate 2 (Figure 7, *bottom*). Table 1 summarizes the computational effort required by the direct FEM and the one-way and two-way SPM.

5. Conclusion

The proposed correction scheme of TS models via a SPM in **two-way** coupling leads to accurate field and current distributions in critical regions, the edges of plates, and so of the ensuing forces and Joules distributions. In particular, SPs in the SPM allow users to use previous local meshes instead of starting a new complete mesh for any position of the plate. This can drastically reduce the overall computation time when many variations of the problem have to be solved e.g. optimization problems.

REFERENCES

[1] C. Geuzaine, P. Dular, and W. Legros, "Dual formulations for the modeling of thin electromagnetic shells using edge elements", *IEEE Trans. Magn.,* vol. 36, no. 4, pp. 799–802, 2000.

[2] T. Le-Duc, G. Guerin, O. Chadebec, and J.-M Guichon "A new integral formulation for eddy current computation in thin conductive shells", *IEEE Trans. Magn*., vol. 48, no. 2, pp. 427–430, 2012.

[3] Vuong Q. Dang, P. Dular, R.V. Sabariego, L. Krähenbühl, C. Geuzaine, "Subproblem approach for Thin Shell Dual Finite Element Formulations", *IEEE Trans. Magn*., vol. 48, no. 2, pp. 407–410, 2012.

[4] Vuong. Dang Quoc "Calculation of distributions of magnetic fields by a subproblem methods – with application to thin shield models", ISSN 1859-3585 – Hanoi University of Industry, *Journal of Science and Technology,* No 36 (10/2016).

[5] P. Dular, Vuong Q. Dang, R. V. Sabariego, L. Krähenbühl and C. Geuzaine, "Correction of thin shell finite element magnetic models via a subproblem method", *IEEE Trans. Magn*., Vol. 47, no. 5, pp. 158 –1161, 2011.

[6] Patick Dular, Laurent Krähenbühl, Ruth. Sabariego, Mauricio Ferreira da Luz, and Christophe Geuzaine, "A Finite Element Subproblem Method for Position Change Conductor System*", IEEE Trans. Magn.*, vol.48, no. 2, pp. 403-406, 2012.

[7] P. Dular, R. V. Sabariego, M. V. Ferreira da Luz, P. Kuo-Peng and L. Krähenbühl, "Perturbation Finite Element Method for Magnetic Model Refinement of Air Gaps and Leakage Fluxes", *IEEE Trans. Magn.,* vol.45, no. 3, pp. 1400-1403, 2009.

[8] C. Geuzaine, B. Meys, F. Henrotte, P. Dular and W. Legros, "A Galerkin projection method for mixed finite elements", *IEEE Trans. Magn*., Vol. 35, No. 3, pp. 1438-1441, 1999.

[9] P. Dular and R. V. Sabariego, "A perturbation method for computing field distortions due to conductive regions with h-conform magnetodynamic finite element formulations*", IEEE Trans. Magn*., vol. 43, no. 4, pp. 1293-1296, 2007.

(The Board of Editors received the paper on 19/05/2017, its review was completed on 01/08/2017)